arXiv:1411.1642v1 [hep-ph] 6 Nov 2014

BARI-TH/2014-693
November 7, 2014

New Physics Scenarios in $b \to c\ell\overline{\nu}_\ell$ decays

Fulvia De Fazio

Istituto Nazionale di Fisica Nucleare - Sezione di Bari
Via Orabona 4, I-70126 Bari, ITALY

The latest BaBar measurements of the ratios $\mathcal{R}(D^{(*)}) = \dfrac{\mathcal{B}(B \to D^{(*)}\tau\overline{\nu}_\tau)}{\mathcal{B}(B \to D^{(*)}\mu\overline{\nu}_\mu)}$ deviate from the Standard Model predictions at the global level of 3.4σ. A possibility to reproduce these experimental ratios without affecting other modes which do not show similar deviations is to consider new physics scenarios producing an additional tensor operator in the effective weak Hamiltonian. I describe the impact of such an operator in semileptonic $B \to D^{(*)}$ modes and in semileptonic B and B_s decays to excited positive parity charmed mesons. In particular, I discuss the most effective observables able to discriminate new physics from the Standard Model.

PRESENTED AT

8th International Workshop on the CKM Unitarity Triangle
(CKM 2014),
Vienna, Austria, September 8-12, 2014

1 Introduction

Semileptonic decays induced by the $b \to c\ell\overline{\nu}_\ell$ transition are the cleanest modes to measure the element V_{cb} of the Cabibbo-Kobayashi-Maskawa (CKM) matrix. Recently, the possibility to use them to test lepton flavour universality and to reveal new physics (NP) effects emerged, prompted by the BaBar Collaboration results [1]:

$$\begin{aligned}
\mathcal{R}^-(D) &= \frac{\mathcal{B}(B^- \to D^0\tau^-\,\overline{\nu}_\tau)}{\mathcal{B}(B^- \to D^0\ell^-\,\overline{\nu}_\ell)} = 0.429 \pm 0.082 \pm 0.052 \ , \\
\mathcal{R}^-(D^*) &= \frac{\mathcal{B}(B^- \to D^{*0}\tau^-\,\overline{\nu}_\tau)}{\mathcal{B}(B^- \to D^{*0}\ell^-\,\overline{\nu}_\ell)} = 0.322 \pm 0.032 \pm 0.022 \ , \\
\mathcal{R}^0(D) &= \frac{\mathcal{B}(\overline{B}^0 \to D^+\tau^-\,\overline{\nu}_\tau)}{\mathcal{B}(\overline{B}^0 \to D^+\ell^-\,\overline{\nu}_\ell)} = 0.469 \pm 0.084 \pm 0.053 \ , \\
\mathcal{R}^0(D^*) &= \frac{\mathcal{B}(\overline{B}^0 \to D^{*+}\tau^-\,\overline{\nu}_\tau)}{\mathcal{B}(\overline{B}^0 \to D^{*+}\ell^-\,\overline{\nu}_\ell)} = 0.355 \pm 0.039 \pm 0.021
\end{aligned} \tag{1}$$

(the first and second error are the statistic and systematic uncertainty, respectively). As I discuss in the following, the results in (1) globally deviate at 3.4σ level with respect to the Standard Model (SM) predictions [1, 2], and they might be due to new particles with large couplings to the heavier fermions, namely charged scalars contributing to tree-level $b \to c\ell\overline{\nu}$ transitions [2, 3]. However, if such new particles exist, they should also affect the purely leptonic $B^- \to \tau^-\overline{\nu}_\tau$ mode, for which the most recent experimental branching ratio determinations are compatible with the SM prediction [4]. To assess whether the results in (1) are a signal of NP, one should investigate which NP scenario can reproduce them without affecting the leptonic mode. Here, I summarize the analysis in [5] devoted to such an issue.

2 Exclusive $b \to c\ell\overline{\nu}_\ell$ decays

A modification of the SM effective weak Hamiltonian that produces a variation of the ratios (1), leaving the purely leptonic B decays unaffected, is

$$H_{eff} = \frac{G_F}{\sqrt{2}} V_{cb} \left[\overline{c}\gamma_\mu(1-\gamma_5) b\, \overline{\ell}\gamma^\mu(1-\gamma_5)\overline{\nu}_\ell + \epsilon_T^\ell\, \overline{c}\sigma_{\mu\nu}(1-\gamma_5) b\, \overline{\ell}\sigma^{\mu\nu}(1-\gamma_5)\overline{\nu}_\ell \right] \ . \tag{2}$$

G_F is the Fermi constant, and a new tensor operator has been introduced, with the coupling ϵ_T^ℓ assumed to mainly contribute for $\ell = \tau$: $\epsilon_T^{e,\mu} = 0$ and $\epsilon_T \equiv \epsilon_T^\tau$. Physical observables allow us to constrain this coupling.

To compute the branching ratios in (1), the hadronic matrix element of the Hamiltonian (2) between the B and $D^{(*)}$ mesons are required. In the case of $B \to D\ell\overline{\nu}_\ell$,

they can be parameterized in terms of the form factors $F_0(q^2)$, $F_1(q^2)$ for the SM part, and of $F_T(q^2)$, $G_T(q^2)$ for the tensor operator. In the case of $B \to D^* \ell \overline{\nu}_\ell$, the form factors are $A_1(q^2)$,$A_2(q^2)$, $A_0(q^2)$, $V(q^2)$ and $T_0(q^2)$, $T_1(q^2)$, $T_2(q^2)$, $T_3(q^2)$, $T_4(q^2)$ and $T_5(q^2)$, respectively (see [5] for the matrix element parametrization). In the infinite heavy quark mass limit, all those form factors can be related to the Isgur-Wise universal function ξ [6]. In [5] the results in [7] for such relations have been used, which include next to leading order corrections both in $1/m_{b,c}$ and in $\mathcal{O}(\alpha_s)$. Moreover, the experimental results of the BaBar analysis of $B \to D \mu \overline{\nu}_\mu$ [8] and of Belle analysis of $B \to D^* \mu \overline{\nu}_\mu$ [9] have been exploited to fix the parameters of the function ξ. As a result, the SM predictions for the ratios in (1) are: $\mathcal{R}^0(D)\Big|_{SM} = 0.324 \pm 0.022$ and $\mathcal{R}^0(D^*)\Big|_{SM} = 0.250 \pm 0.003$. While the data for $\mathcal{R}^{-,0}(D)$ do not deviate significantly from SM, a discrepancy is found in $\mathcal{R}^{-,0}(D^*)$. In the next section I describe the impact of the new Hamiltonian (2) on these ratios.

3 NP predictions for $\mathcal{R}(D^{(*)})$ and other observables

The inclusion of the new tensor operator in (2) modifies the SM prediction for $\mathcal{R}(D^{(*)})$. Therefore, the coupling ϵ_T can be bound in order to reproduce the results (1); predictions for other observables can be worked out with ϵ_T varying in the obtained region [5]. The experimental constraints bound the region shown in Fig.1. The biggest circle represents the constraint from the $\mathcal{R}(D)$ data, the smaller circle is derived imposing the result for $\mathcal{R}(D^*)$. Adopting the parameterization $\epsilon_T = |a_T| e^{i\theta} + \epsilon_{T0}$, the result depicted in Fig.1 can be written as

$$Re[\epsilon_{T0}] = 0.17\,, \quad Im[\epsilon_{T0}] = 0\ , \quad |a_T| \in [0.24,\, 0.27]\,, \quad \theta \in [2.6,\, 3.7]\,\text{rad}\ . \qquad (3)$$

Several observables can be computed varying ϵ_T in this range [5].

The spectra $d\Gamma(B \to D^{(*)} \tau \overline{\nu}_\tau)/dq^2$ (summed over the D^* polarizations) have been measured by BaBar [10] and compared to SM predictions, arguing that the SM distributions are compatible with data. Fig.2 shows that there is compatibility also in the NP scenario discussed here, therefore the shape of the decay spectra is not effective to discriminate between the two possibilities. Observables showing more significant deviations from the SM predictions are the D^* longitudinal (L) and transverse (T) polarization fractions $F_{L,T}(q^2) = \frac{d\Gamma_{L,T}(B \to D^* \tau \overline{\nu}_\tau)}{dq^2} \times \left(\frac{d\Gamma(B \to D^* \tau \overline{\nu}_\tau)}{dq^2}\right)^{-1}$. In SM, $F_L(q^2)$ ranges between 0.75 at low q^2 and about 0.35 at high q^2; in NP, with ϵ_T in the region (3), $F_L(q^2)$ varies between 0.35 and about 0.65 at low q^2, converging to the SM value at high q^2. While in the SM the longitudinal F_L dominates at small q^2, in NP F_L and F_T have similar size up to $q^2 = 6$ GeV^2.

A very sensitive observable is the forward-backward $\mathcal{A}_{FB}(q^2)$ asymmetry in $B \to$

$D\tau\overline{\nu}_\tau$ and $B \to D^*\tau\overline{\nu}_\tau$. It is defined as

$$\mathcal{A}_{FB}(q^2) = \frac{\int_0^1 d\cos\theta_\ell \frac{d\Gamma}{dq^2 d\cos\theta_\ell} - \int_{-1}^0 d\cos\theta_\ell \frac{d\Gamma}{dq^2 d\cos\theta_\ell}}{\frac{d\Gamma}{dq^2}} \ , \tag{4}$$

θ_ℓ being the angle between the direction of the τ and the $D^{(*)}$ in the rest frame of the lepton pair. Fig.3 shows $\mathcal{A}_{FB}(q^2)$ for $B \to D^*\tau\overline{\nu}_\tau$. The SM prediction is affected by a tiny theoretical uncertainty, since the dependence on the hadronic form factors reduces in the ratio. In the case of NP, the prediction takes into account also the uncertainty on θ and $|a_T|$. The SM curve lies below the NP distribution for all values of q^2. Interestingly, the SM predicts a zero for $\mathcal{A}_{FB}$ at $q^2 \simeq 6.15$ GeV^2, while in the NP case the zero is shifted towards larger values: $q^2 \in [8.1, 9.3]$ GeV^2. Therefore,

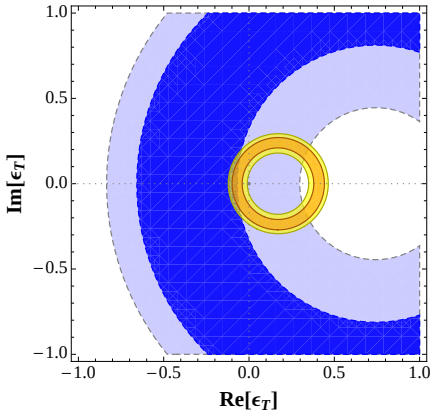

Figure 1: Region in the plane $(Re(\epsilon_T), Im(\epsilon_T))$ determined from the experimental data in (1) on $\mathcal{R}(D)$ (large rings) and $\mathcal{R}(D^*)$ (small rings). The inner and outer circles correspond to 1σ and 2σ, respectively.

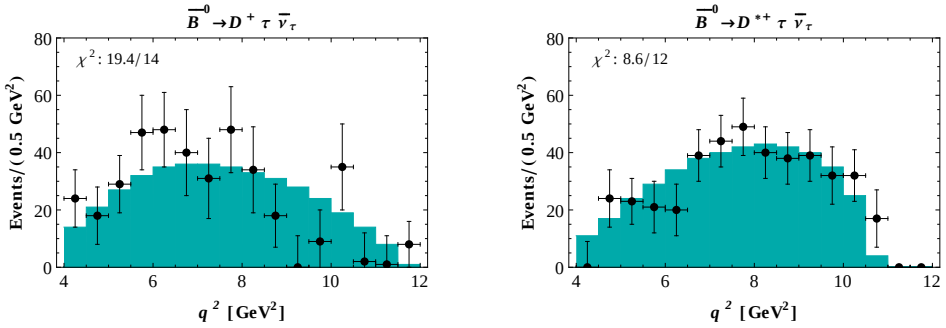

Figure 2: $\dfrac{d\Gamma(B \to D\tau\overline{\nu}_\tau)}{dq^2}$ (left) and $\dfrac{d\Gamma(B \to D^*\tau\overline{\nu}_\tau)}{dq^2}$ (right) distributions in the NP scenario (for the central value of ϵ_T, shaded histograms), compared to the BaBar data (points) [10]. The distributions are normalized to the total number of events.

although the experimental determination of the zero of $\mathcal{A}_{FB}(q^2)$ is a challenging task, this observable can discriminate SM from NP.

4 Role of the tensor operator in $B \to D^{**}\ell\overline{\nu}_\ell$ decays

The new operator in the effective Hamiltonian (2) affects other exclusive decay modes, in particular the semileptonic B and B_s transitions into excited charmed mesons. In the heavy quark limit, the lightest of such hadrons, generically denoted as $D^{**}_{(s)}$, can be classified in doublets: $(D^*_{(s)0},\, D'_{(s)1})$ have spin-parity $J^P = (0^+, 1^+)$; $(D_{(s)1},\, D^*_{(s)2})$ have $J^P = (1^+, 2^+)$. All these mesons, with and without strangeness, have been observed with features fulfilling the theoretical expectations [11]. The tensor operator affects the ratios $\mathcal{R}(D^{**}) = \dfrac{\mathcal{B}(B \to D^{**}\tau\,\overline{\nu}_\tau)}{\mathcal{B}(B \to D^{**}\ell\,\overline{\nu}_\ell)}$ with $D^{**} = D^*_0,\, D'_1,\, D_1,\, D^*_2$, as well as the analogous ratios for $B_s \to D^{**}_s\ell\overline{\nu}_\ell$ transitions (the form factors are taken in the $SU(3)_F$ symmetry limit). In the heavy quark limit, the semileptonic B decays to D^{**} in the same doublet can be described in terms of a single universal function. In the case of B decays to $(D^*_0,\, D'_1)$ such a function is denoted as $\tau_{1/2}(w)$, for B decays to $(D_1,\, D^*_2)$ by $\tau_{3/2}(w)$ (with $q^2 = m_B^2 + m_{D^{**}}^2 - 2m_B m_{D^{**}} w$). Several theoretical determinations of $\tau_i(w)$ exist in the literature: in [5] a QCD sum rule determination of $\tau_{3/2}(w)$ at leading order in α_s [12], and of $\tau_{1/2}(w)$ at $\mathcal{O}(\alpha_s)$ [13] have been used. The correlations between the ratios $\mathcal{R}(D^{**})$ for B and B_s decays are displayed in Fig.4, together with the SM predictions: $(\mathcal{R}(D^*_0), \mathcal{R}(D'_1)) = (0.077, 0.100)$, $(\mathcal{R}(D^*_{s0}), \mathcal{R}(D'_{s1})) = (0.107, 0.112)$, $(\mathcal{R}(D_1), \mathcal{R}(D^*_2) = (0.065, 0.059)$ and $(\mathcal{R}(D_{s1}), \mathcal{R}(D^*_{s2}) = (0.060, 0.055)$. The tensor operator produces an increase of the ratios $\mathcal{R}$, correlated for the two states in each doublet. The results are rather stable when different models for the τ functions are used, namely those in [14, 15]. Also in the case of final states with D^{**} mesons, sensitive observables are the forward-backward asymmetries. The most interesting ones

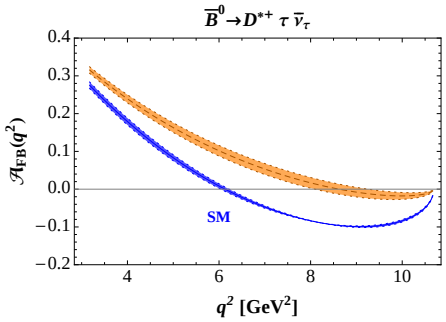

Figure 3: $\mathcal{A}_{FB}(q^2)$ for $B \to D^*\tau\overline{\nu}_\tau$. The lower (blue) curve is the SM prediction, the upper (orange) band the NP expectation. Uncertainty on the form factor parameters has been included and, in the case of NP, also on the parameters $|a_T|$ and θ.

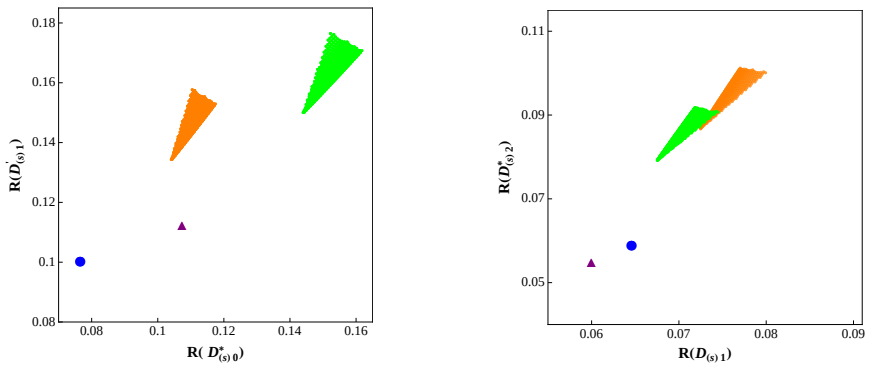

Figure 4: Correlation between $\mathcal{R}(D^*_{(s)0})$, $\mathcal{R}(D'_{(s)1})$ (left) and $\mathcal{R}(D_{(s)1})$, $\mathcal{R}(D^*_{(s)2})$ (right). Orange, dark (gree, light) regions refer to mesons without (with) strangeness. The dots (triangles) are the SM results for mesons without (with) strangeness.

are obtained in the case of D'_1 and D^*_2, Fig.5. When the tensor operator is included, the asymmetries $\mathcal{A}_{FB}$ are enhanced with respect to SM for all values of q^2. Moreover, the zero of the asymmetries, that is present in both cases in SM, is shifted towards larger values of q^2 in $B \to D'_1 \tau \overline{\nu}_\tau$, and disappears in the case of $B \to D^*_2 \tau \overline{\nu}_\tau$.

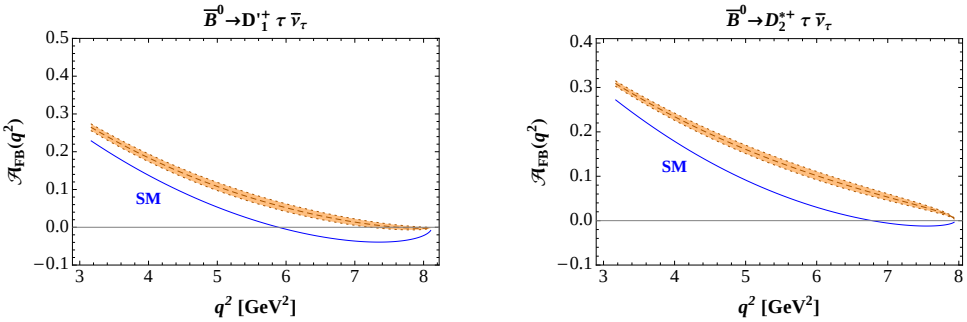

Figure 5: $\mathcal{A}_{FB}(q^2)$ for $B \to D'_1 \tau \overline{\nu}_\tau$ (left), and $B \to D^*_2 \tau \overline{\nu}_\tau$ (right) . The solid (blue) curves are the SM predictions, the dotted (orange) bands the NP expectations.

5 Conclusions

A possibility to explain the ratios in (1), leaving $B \to \tau \overline{\nu}_\tau$ unaffected, is an additional tensor operator in the effective $b \to c\ell\nu$ Hamiltonian. Its coupling ϵ_T has been constrained using experimental data and employed to compute several observables. The most sensitive one to discriminate the NP scenario from SM is the forward-backward asymmetry in $B \to D^* \tau \overline{\nu}_\tau$, with a shift in the position of its zero. In the case of B decays to excited charmed mesons, the NP model predicts an enhancement

of the ratios $\mathcal{R}$ with respect to SM and a sizable modification of the forward-backward asymmetries in the decays to D_1' and D_2^*.

ACKNOWLEDGEMENTS

I thank P. Biancofiore and P. Colangelo for collaboration on the topics discussed here.

References

[1] J. P. Lees *et al.* [BaBar Collaboration], Phys. Rev. Lett. **109**, 101802 (2012).

[2] S. Fajfer, J. F. Kamenik and I. Nisandzic, Phys. Rev. D **85**, 094025 (2012).

[3] S. Fajfer *et al.*, Phys. Rev. Lett. **109**, 161801 (2012); A. Crivellin *et al.*, Phys. Rev. D **86**, 054014 (2012); Phys. Rev. D **87**, no. 9, 094031 (2013); A. Datta *et al.*, Phys. Rev. D **86**, 034027 (2012); D. Becirevic *et al.*, Phys. Lett. B **716**, 208 (2012); A. Celis *et al.*, JHEP **1301**, 054 (2013); D. Choudhury *et al.*, Phys. Rev. D **86**, 114037 (2012); M. Tanaka and R. Watanabe, Phys. Rev. D **87**, 034028 (2013); I. Dorner *et al*, JHEP **1311**, 084 (2013); Y. Sakaki *et al*, Phys. Rev. D **88**, no. 9, 094012 (2013); M. Duraisamy *et al*, Phys. Rev. D **90**, 074013 (2014).

[4] I. Adachi *et al.* [Belle Collaboration], Phys. Rev. Lett. **110**, no. 13, 131801 (2013); J. P. Lees *et al.* [BaBar Collaboration], Phys. Rev. D **88**, no. 3, 031102 (2013).

[5] P. Biancofiore, P. Colangelo and F. De Fazio, Phys. Rev. D **87**, 074010 (2013).

[6] N. Isgur and M. B. Wise, Phys. Lett. B **237**, 527 (1990).

[7] I. Caprini, L. Lellouch and M. Neubert, Nucl. Phys. B **530**, 153 (1998).

[8] B. Aubert *et al.* [BABAR Collaboration], Phys. Rev. Lett. **104**, 011802 (2010).

[9] W. Dungel *et al.* [Belle Collaboration], Phys. Rev. D **82**, 112007 (2010).

[10] J. P. Lees *et al.* [The BaBar Collaboration], Phys. Rev. D **88**, 072012 (2013).

[11] P. Colangelo *et al.*, Phys. Rev. D **86**, 054024 (2012).

[12] P. Colangelo, G. Nardulli and N. Paver, Phys. Lett. B **293**, 207 (1992); P. Colangelo, F. De Fazio and N. Paver, Nucl. Phys. Proc. Suppl. **75B**, 83 (1999).

[13] P. Colangelo, F. De Fazio and N. Paver, Phys. Rev. D **58**, 116005 (1998).

[14] V. Morenas *et al*, Phys. Rev. D **56**, 5668 (1997).

[15] B. Blossier *et al.* [European Twisted Mass Collab.], JHEP **0906**, 022 (2009).